Thermal characterization of electrical tracing-assisted dual-microring optical sensors

Qing Liu,[1*] Kyung Woo Kim,[1] Jack Sheng Kee,[1] Junfeng Song,[1,2] Guo-Qiang Lo,[1] and Mi Kyoung Park[1]

[1]*Institute of Microelectronics, A*STAR (Agency for Science, Technology and Research), 11 Science Park Road, Singapore Science Park II, 117685, Singapore*

[2]*State Key Laboratory on Integrated Opto-Electronics, College of Electronic Science and Engineering, Jilin University, Changchun 130012, China*

[*]*liuq@ime.a-star.edu.sg*

Abstract: In this paper, we study the temperature sensitivity of an electrical tracing-assisted dual-microring optical sensor, which consists of a sensing ring to detect the refractive index change on its surface and a tracing ring to trace the resonance wavelength shift of the sensing ring by the thermo-optic effect with a heating electrode on it. The wavelength shift measurement is therefore changed to electrical power variation measurement. Thanks to the real-time compensation effect of the tracing ring, the temperature dependence of the sensor is found to be intrinsically low. The resonance wavelength temperature sensitivity difference between the two rings is measured to be as low as 10.1 pm/°C, showing that the temperature dependence of the sensor in terms of wavelength per degree is reduced by ~6 times compared to that of a single ring sensor. The temperature sensitivity of the sensor in terms of electrical power per degree is measured to be −0.077 mW/°C. By using tracing ring with enhanced tuning efficiency, this value can be further decreased to −0.0057 W/°C. The experimental results agree well with the expectation. This type of sensors with low temperature dependence has great potential to be deployed in various practical point-of-care diagnostic applications.

©2014 Optical Society of America

OCIS codes: (280.1415) Biological sensing and sensors; (280.4788) Optical sensing and sensors; (130.3120) Integrated optics devices; (130.6010) Sensors.

References and links

1. X. D. Fan, I. M. White, S. I. Shopova, H. Y. Zhu, J. D. Suter, and Y. Z. Sun, "Sensitive optical biosensors for unlabeled targets: a review," Anal. Chim. Acta **620**(1-2), 8–26 (2008).
2. M. Iqbal, M. A. Gleeson, B. Spaugh, F. Tybor, W. G. Gunn, M. Hochberg, T. Baehr-Jones, R. C. Bailey, and L. C. Gunn, "Label-free biosensor arrays based on silicon ring resonators and high-speed optical scanning instrumentation," IEEE J. Sel. Top. Quantum Electron. **16**(3), 654–661 (2010).
3. D.-X. Xu, M. Vachon, A. Densmore, R. Ma, A. Delâge, S. Janz, J. Lapointe, Y. Li, G. Lopinski, D. Zhang, Q. Y. Liu, P. Cheben, and J. H. Schmid, "Label-free biosensor array based on silicon-on-insulator ring resonators addressed using a WDM approach," Opt. Lett. **35**(16), 2771–2773 (2010).
4. K. De Vos, I. Bartolozzi, E. Schacht, P. Bienstman, and R. Baets, "Silicon-on-Insulator microring resonator for sensitive and label-free biosensing," Opt. Express **15**(12), 7610–7615 (2007).
5. T. Claes, J. G. Molera, K. De Vos, E. Schacht, R. Baets, and P. Bienstman, "Label-free biosensing with a slot-waveguide-based ring resonator in silicon on insulator," IEEE Photonics Journal **1**(3), 197–204 (2009).
6. J. Song, X. Luo, X. Tu, M. K. Park, J. S. Kee, H. Zhang, M. B. Yu, G.-Q. Lo, and D.-L. Kwong, "Electrical tracing-assisted dual-microring label-free optical bio/chemical sensors," Opt. Express **20**(4), 4189–4197 (2012).
7. K. W. Kim, J. Song, J. S. Kee, Q. Liu, G.-Q. Lo, and M. K. Park, "Label-free biosensor based on an electrical tracing-assisted silicon microring resonator with a low-cost broadband source," Biosens. Bioelectron. **46**, 15–21 (2013).
8. J. Song, X. Luo, J. S. Kee, K. Han, C. Li, M. K. Park, X. Tu, H. Zhang, Q. Fang, L. Jia, Y.-J. Yoon, T.-Y. Liow, M. B. Yu, and G.-Q. Lo, "Silicon-based optoelectronic integrated circuit for label-free bio/chemical sensor," Opt. Express **21**(15), 17931–17940 (2013).
9. G. Cocorullo, F. Della Corte, and I. Rendina, "Temperature dependence of the thermo-optic coefficient in crystalline silicon between room temperature and 550 K at the wavelength of 1523 nm," Appl. Phys. Lett. **74**(22), 3338–3340 (1999).

#220696 - $15.00 USD Received 11 Aug 2014; revised 18 Sep 2014; accepted 19 Sep 2014; published 23 Oct 2014

10. M. S. Nawrocka, T. Liu, X. Wang, and R. R. Panepucci, “Tunable silicon microring resonator with wide free spectral range,” Appl. Phys. Lett. **89**(7), 071110 (2006).
11. Y. Shin, A. P. Perera, K. W. Kim, and M. K. Park, “Real-time, label-free isothermal solid-phase amplification/detection (ISAD) device for rapid detection of genetic alteration in cancers,” Lab Chip **13**(11), 2106–2114 (2013).
12. M. K. Park, Q. Liu, K. W. Kim, Y. Shin, J. S. Kee, J. F. Song, G.-Q. Lo, and D. L. Kwong, “Integrated silicon microring resonator devices for point-of-care diagnostic applications,” Proc. SPIE **8990**, 89900V (2014).
13. D.-X. Xu, M. Vachon, A. Densmore, R. Ma, S. Janz, A. Delâge, J. Lapointe, P. Cheben, J. H. Schmid, E. Post, S. Messaoudène, and J. M. Fédéli, “Real-time cancellation of temperature induced resonance shifts in SOI wire waveguide ring resonator label-free biosensor arrays,” Opt. Express **18**(22), 22867–22879 (2010).
14. H. El-Kashef, “The necessary requirements imposed on polar dielectric laser dye solvents–II,” Physica B **311**(3-4), 376–379 (2002).
15. Q. Fang, J. Song, X. Luo, L. Jia, M. Yu, G.-Q. Lo, and Y. Liu, “High efficiency ring-resonator filter with NiSi heater,” IEEE Photon. Technol. Lett. **24**(5), 350–352 (2012).

1. Introduction

The demand for low-cost, highly sensitive and compact optical sensors has been increasing rapidly in a number of applications such as medical diagnosis and environmental monitoring [1]. Among the existing sensors, silicon-on-insulator (SOI) ring resonator sensor has been attracting much of research interests due to its compactness, robustness, high sensitivity and compatibility with complementary metal-oxide-semiconductor (CMOS) technology. Single SOI ring resonator sensors have been demonstrated in both conventional waveguides and slot-waveguide, with detection limit from 10^{-4}~10^{-7} RIU (refractive index unit) [2–5]. The wavelength-scanning method is widely used for ring resonator optical sensing interrogation and there are two ways involving different equipments. One way is to use a wavelength-tunable laser as the light source and a photodetector for light detection, while the other way is to use a broadband light source together with an optical spectrum analyzer (OSA) for wavelength interrogation. To achieve low limit of detection (LOD), it requires high-resolution wavelength-tunable light source or OSA, which are expensive and not suitable for the development of low-cost and portable optical biosensing system for point-of-care (POC) applications.

Recently a new type of electrical tracing-assisted dual-microring optical sensor by integrating various electrical and photonic devices in a single silicon chip has been proposed and demonstrated [6]. The dual-microring sensor consists of a sensing ring to detect the refractive index change on its surface and a tracing ring to trace the resonance wavelength shift of the sensing ring by the thermo-optic (TO) effect with a heating electrode on it. The wavelength shift measurement is therefore changed to electrical power variation measurement. The cheaper broadband light source (amplified spontaneous emission (ASE) or light-emitting diode (LED)) can be used instead of a high-resolution wavelength-tunable laser. Besides the advantage of potential lower cost, such sensing system can also provide relatively low LOD due to the novel sensing interrogation by obtaining the refractive index change from the applied electrical power [6]. The first proof-of-principle demonstration was done by testing the deposition of polyelectrolyte multilayer $(PSS/PAH)_N$, showing surface sensitivity of ~4.0 mW/ng·mm^{-2} and a detection limit of ~5.35 pg/mm^2 [6]. The sensor was then successfully demonstrated for quantitative and specific detection of a well-known breast cancer biomarker (human epidermal growth factor receptor 2 (HER2)) in a bovine serum albumin solution [7]. Recently, by replacing the power meter with an on-chip Ge photodetector, bulk sensitivity of 15 mW/RIU and surface mass sensitivity of 192 μW/ng·mm^{-2} have been achieved, which correspond to detection limits of 3.9 μ-RIU and 0.3 pg/mm^2, respectively [8].

Practical sensors for assay and molecular binding measurements must be robust and immune to external environmental changes. One of the most commonly encountered problems is temperature drift. The working principle of the ring resonator sensor is generally based on the measurement of the resonance wavelength shift. However, its resonance wavelength also shifts as the temperature changes. Therefore, temperature drift during the measurement induces wavelength shift which can be superimposed onto the useful real wavelength shift and decreases the sensing accuracy and stability. In particular, due to the high TO coefficient of silicon (1.86×10^{-4} K^{-1} [9]), the silicon ring resonators are typically highly susceptible to fluctuations in temperature [10]. In addition, for certain biochemical sensing applications, such as real-time on-chip nucleic acid amplification reaction, active temperature control is required and both temperature variation and control accuracy affect the detection results [11,12]. Although external heaters or coolers can be employed to stabilize the chip temperature, they require extra space and power. Therefore the thermal property of the SOI ring resonator sensors needs to be characterized before use and low temperature dependence is desirable. In this paper, we study the temperature sensitivity of this new electrical tracing-assisted dual-microring optical sensor for the first time. Its temperature sensitivity is found to be intrinsically low because the resonance wavelength temperature dependence of the sensing ring is compensated by that of the tracing ring. Compared with the additional reference ring added to cancel the temperature-induced resonance wavelength shift of the sensing ring in [13], the tracing ring in the dual-microring sensor not only changes the wavelength shift measurement to electrical power variation measurement but also compensates for temperature dependence of the sensing ring in a real-time manner. The measurement results are already temperature compensated and no data processing is needed.

2. Sensor working principle and temperature sensitivity analysis

Figure 1 shows the design layout of the electrical tracing-assisted dual-microring sensor, which consists of two serially cascaded ring resonators [6]. The left lower ring with its upper cladding etched away detects the refractive index change on the ring surface and is denoted as the sensing ring. For biochemical sensing applications, its resonance wavelength shifts as the bimolecular binding occurs on it. The right upper ring actively traces the resonance wavelength shift of the sensing ring by a heating electrode on it and is denoted as the tracing ring. By control of the electrical power applied to the electrode, the generated heat shifts the resonance wavelengths of the tracing ring by the TO effect. The wavelength shift $\Delta\lambda_t$ is proportional to the applied electrical power P and can be obtained as

$$\Delta\lambda_t = AP, \tag{1}$$

where A is the TO (or electrical tuning) efficiency of the tracing ring.

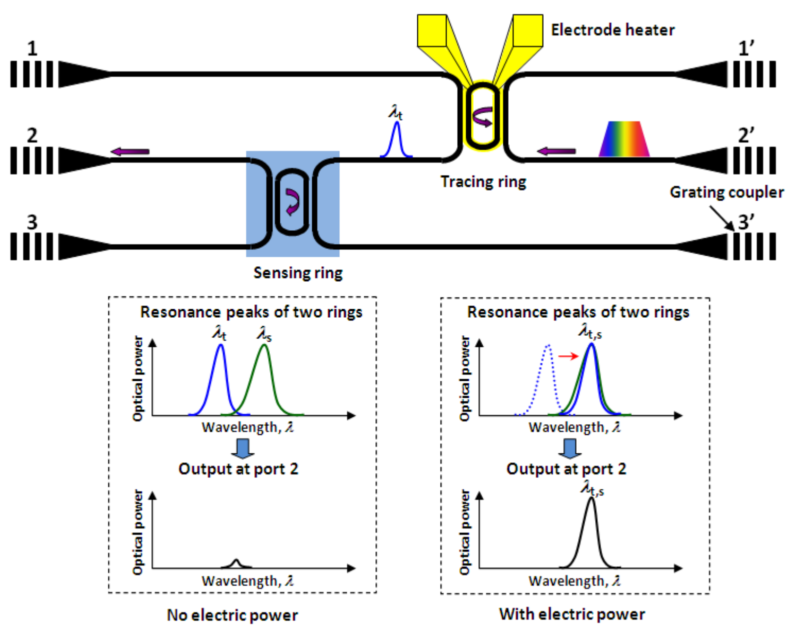

Fig. 1. Design layout of the electric tracing-assisted dual-microring optical sensor.

#220696 - $15.00 USD Received 11 Aug 2014; revised 18 Sep 2014; accepted 19 Sep 2014; published 23 Oct 2014
(C) 2014 OSA

As shown in Fig. 1, a broadband light coupled into input-port 2' goes through the tracing ring and feeds into the sensing ring from a drop-port of the tracing ring. Limiting the wavelength range of the broadband light source to be less than one free-spectral range (FSR), there is only one resonance peak for each ring (λ_t for tracing ring and λ_s for sensing ring as shown in Fig. 1). Without applying any electrical power, the resonance peaks of the sensing ring and the tracing ring are separated from each other and there is no overlap between their resonance bands; therefore, the output optical power at port 2 is minimized. The overlap between the two resonance bands as well as the optical power at the output-port 2 reaches maximum only when both resonance peaks align with each other (filter-cascading effect). By scanning the electrical power applied to the tracing ring while monitoring the output optical power, the required electrical power for the tracing ring to align with the sensing ring can be obtained. As the resonance wavelength of the sensing ring shifts to a new position due to the bimolecular binding on its surface, the electrical power required for the tracing ring to align with the sensing ring changes accordingly. Therefore, the resonance wavelength shift of the sensing ring can be indirectly extracted by monitoring the required electrical power change on the tracing ring to achieve maximum output optical power at output-port 2. The wavelength shift measurement is therefore changed to electrical power variation measurement. Since the required electrical power P to trace the sensing ring is proportional to the resonance peak separation between the two rings $\lambda_s - \lambda_t$, the temperature sensitivity of the sensor is derived as

$$\frac{dP}{dT} = \frac{1}{A}\left(\frac{d\lambda_s}{dT} - \frac{d\lambda_t}{dT}\right) - \frac{P_0}{A}\frac{dA}{dT}, \tag{2}$$

where $P_0 = (\lambda_s - \lambda_t)/A$. $d\lambda_s/dT$ and $d\lambda_t/dT$ are the resonance wavelength temperature sensitivity of the sensing ring and tracing ring, respectively. Equation (2) gives how much electrical power is required for the tracing ring to align with the sensing ring as the temperature changes. We will show later that A depends weakly on the temperature and the second term on the right side of Eq. (2) is small. The temperature sensitivity of the sensor is mainly decided by the resonance wavelength temperature sensitivity difference between the two rings ($d\lambda_s/dT - d\lambda_t/dT$), and the electrical tuning efficiency of the tracing ring (A). According to Eq. (2), the temperature-induced resonance wavelength shift for the sensing ring is compensated by that of the tracing ring, and the temperature sensitivity of this dual-microring sensor is intrinsically low when both rings have similar resonance wavelength temperature dependence.

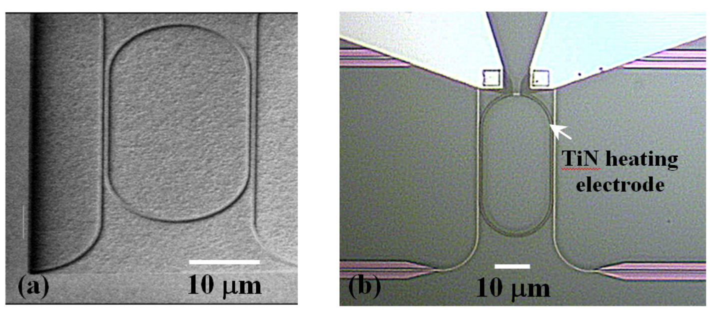

Fig. 2. (a) SEM image of a sensing ring where the upper oxide cladding is etched away. (b) Microscopic image of a tracing ring where TiN heating electrode is placed on the ring.

3. Sensor fabrication and optical setup

The sensor was fabricated using standard CMOS processes. The fabrication was started on a commercially available 200 mm SOI wafer with a 220 nm-thick top silicon layer and a 2 μm-thick buried oxide (BOX) layer. First, the ring structures were patterned using 248-nm deep UV lithography and etched to the BOX using the reactive ion etching (RIE) process. The

#220696 - $15.00 USD Received 11 Aug 2014; revised 18 Sep 2014; accepted 19 Sep 2014; published 23 Oct 2014
(C) 2014 OSA

silicon waveguide was 500 nm wide and the coupling length and coupling gaps between side-coupled waveguide and rings were 20 μm and 400 nm, respectively. Both rings were designed identically with 10 μm radius. Then 1.1 μm of oxide was deposited, followed by 150 nm titanium nitride (TiN) deposition for the thermal heater. The width of the heater strip was 1 μm. Next, 50 nm-thick silicon nitride was deposited for TiN etching protection. After the formation of contact holes, ~750 nm thick aluminum was deposited, followed by metal pad etching. Finally, the sensing window was opened for the sensing ring using reactive ion etching and wet etching, respectively. Figures 2(a) and 2(b) show the SEM and microscopic images of the fabricated sensing and tracing rings.

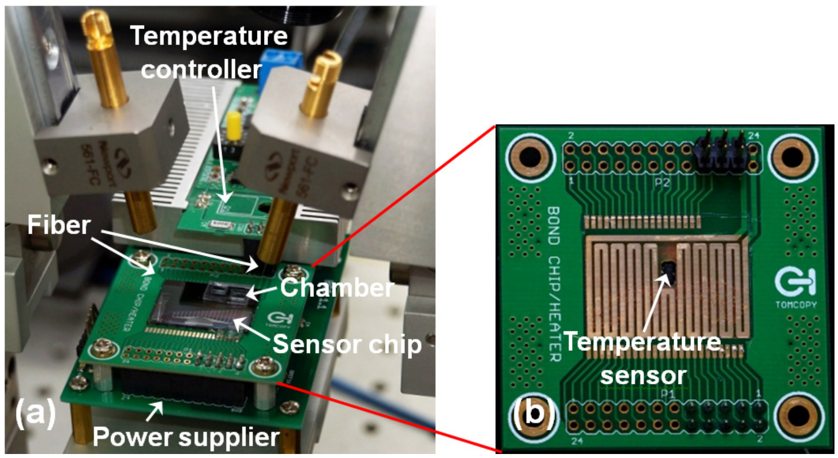

Fig. 3. Images of the (a) experimental setup and the (b) thermal heater placed under the chip.

In the measurement of the dual-microring system, a C-band ASE light source (Opto-Link Corp. Ltd., Hong Kong) and a tunable band-pass filter (Alnair Labs, BVF-200, Tokyo, Japan) were used together to generate light waves with desired bandwidth. The experimental setup is shown in Fig. 3(a). The light was coupled into the sensor chip through a vertical grating coupler. The output light was coupled to a single mode fiber through another grating coupler and detected with an optical power meter (Agilent 81634B, Santa Clara, CA, USA). The chip was placed on a printed circuit (PCB) board with a thermal heater and a temperature sensor on its surface as shown in Fig. 3(b). The PCB board was connected with a temperature controller on one side to control the temperature of the whole chip. A custom-made power supplier was placed under the PCB board to supply the electrical power to the tracing ring. Both the power meter and the power supplier are remotely controlled through a computer interface developed in our laboratory using the LabVIEW program. The output optical power was recorded while scanning the electrical power over a given range and the electrical power value at the maximum optical power was recorded in real time. The optical transmission spectra of the tracing ring and sensing ring were obtained by launching light into the input ports 3′ and measuring the output ports at 1 with the EXFO IQS-12004B DWDM passive component test system (with a wavelength accuracy of 5pm). Open chamber made from 0.2-μm thick double-side plastic tape was placed on the sensing ring and the deionized (DI) water was used as test solution.

4. Temperature sensitivity measurement

We first studied the resonance wavelength temperature sensitivity of the tracing ring and sensing ring, from which we obtained their sensitivity difference. Then we measured the electrical tuning efficiency of the tracing ring at different temperatures. Finally, we characterized the temperature sensitivity of the dual-microring sensor in terms of electrical power per degree.

#220696 - $15.00 USD Received 11 Aug 2014; revised 18 Sep 2014; accepted 19 Sep 2014; published 23 Oct 2014
(C) 2014 OSA

Figure 4(a) shows the transmission spectra for the tracing ring and sensing ring measured at several temperatures. The dependence of the resonance wavelength of the tracing ring and sensing ring and their separation on the temperature are shown in Fig. 4(b). The resonance wavelengths of both rings shift to longer wavelength as temperature increases and their temperature sensitivity is linearly fitted to be 69.5 pm/°C and 59.4 pm/°C, respectively. The negative TO coefficient of water (-1.2×10^{-4} K^{-1} [14],) results in sensing ring's reduced temperature sensitivity compared to that for the tracing ring with an oxide upper cladding. The tracing ring shifts faster than the sensing ring and their resonance wavelength temperature sensitivity difference (sensing ring minus tracing ring) is −10.1 pm/°C as shown in Fig. 4(b). Thanks to the compensation effect of the tracing ring, the temperature sensitivity of this dual-microring sensor in terms of wavelength per degree is reduced by almost 6 times compared to that of a single ring sensor.

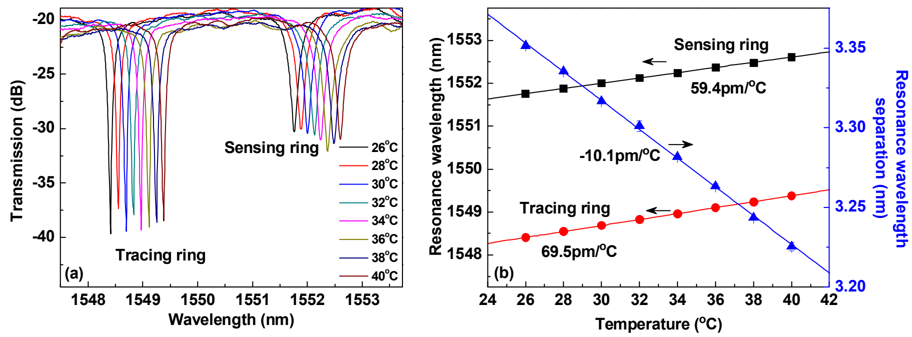

Fig. 4. (a) Transmission spectra for the tracing ring and sensing ring measured at different temperatures. (b) Dependence of the resonance wavelength of the tracing ring and sensing ring and their separation on the temperature.

We then studied the temperature dependence of the electrical tuning efficiency of the tracing ring. We measured the variation of its resonance wavelength with the applied electrical power at different temperatures. The results are shown in Fig. 5(a) and corresponding electrical tuning efficiency A is summarized in Fig. 5(b). The average of electrical tuning efficiency at eight different temperatures is ~152.2 pm/mW and it has weak temperature dependence of $\sim 6.64 \times 10^{-2}$ pm/(mW· °C) by linear fitting.

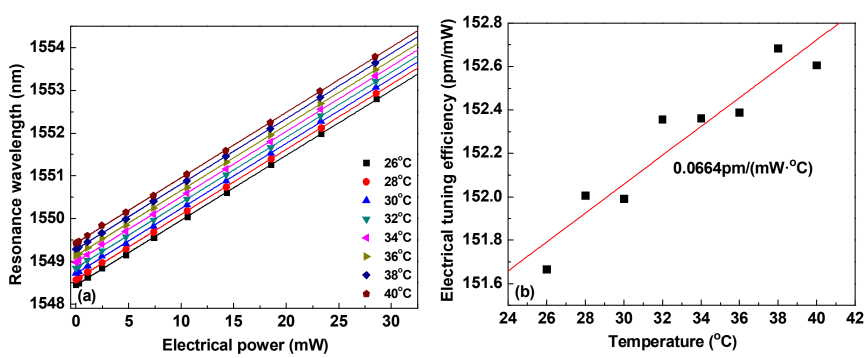

Fig. 5. (a) Resonance wavelength of the tracing ring as a function of the applied electrical power measured at different temperatures. (b) Dependence of the electrical tuning efficiency of the tracing ring on the temperature.

#220696 - $15.00 USD Received 11 Aug 2014; revised 18 Sep 2014; accepted 19 Sep 2014; published 23 Oct 2014
(C) 2014 OSA 3 November 2014 | Vol. 22, No. 22 | DOI:10.1364/OE.22.027069 | OPTICS EXPRESS 27074

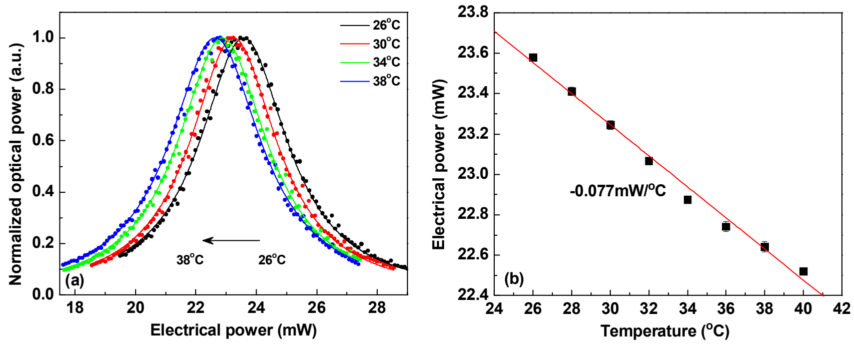

Fig. 6. (a) Normalized output optical power as a function of the applied electrical power at different temperatures. (b) Dependence of the electrical power required for achieving maximum output optical power on the temperature.

To study the temperature sensitivity of the dual-microring sensor in terms of electrical power per degree, light was launched into port 2' and the output from port 2 was monitored by the power meter directly. The output optical power was recorded when scanning the applied electrical power on the tracing ring. Each scan was repeated ten times. All scans were done at eight different chip temperatures from 26°C to 40°C. The scanning and fitted (solid lines) results for four temperatures are shown in Fig. 6(a). The average electrical power values corresponding to the maximum output optical power at different temperatures are summarized in Fig. 6(b), where the sensitivity is linearly fitted to be −0.077 mW/°C. This value means 0.077 mW electrical power is required for the tracing ring to align with the sensing ring as the temperature decreases by one degree. This sensitivity can also be obtained from Eq. (2) using the measured resonance wavelength temperature sensitivity of the two rings ($d\lambda_s/dT$, $d\lambda_t/dT$), TO efficiency (A) of the tracing ring and its temperature dependence (dA/dT), all of which are listed in Table 1. The calculated sensitivity is −0.076 mW/°C, which agrees well with the measured value. Since the electrical tuning efficiency of the tracing ring varies slowly with temperature, the contribution from the second item in Eq. (2) is small (~−0.01 mW/°C). The temperature sensitivity is therefore mainly decided by the first item of Eq. (2), i.e., resonance wavelength temperature sensitivity difference between the two rings and the electrical tuning efficiency of the tracing ring.

Table 1. Calculation of temperature sensitivity.

$d\lambda_s/dT$ (pm/°C)	$d\lambda_t/dT$ (pm/°C)	A (pm/mW)	dA/dT (pm/(mW·°C))	P_0 (mW)	dP/dT (Eq. (2)) (mW/°C)	dP/dT (measured) (mW/°C)
59.4	69.5	152.2	0.0664	23.0	−0.076	−0.077

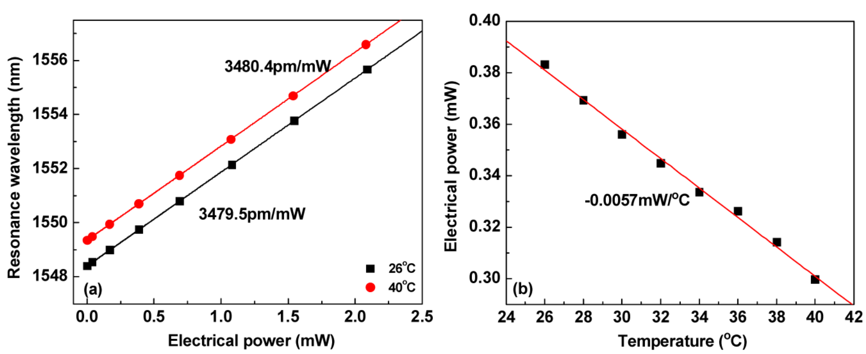

Fig. 7. (a) Resonance wavelength of the tracing ring with enhanced electrical tuning efficiency as a function of the applied electrical power measured at 26°C and 40°C. (b) Dependence of the electrical power required for achieving maximum output optical power on the temperature.

#220696 - $15.00 USD Received 11 Aug 2014; revised 18 Sep 2014; accepted 19 Sep 2014; published 23 Oct 2014
(C) 2014 OSA

5. Discussion and conclusion

According to Eq. (2), the temperature sensitivity of the dual-microring sensor can be reduced further by use of electrode heater with higher electrical tuning efficiency. An electrode heater with much higher electrical tuning efficiency can be realized by using isolation trenches [8,15]. The silicon substrate of the tracing ring is etched away to efficiently confine the generated heat and therefore lowers the electrical power consumption and enhances the electrical tuning efficiency significantly [15]. Figure 7(a) shows the electrical tuning efficiency of the fabricated tracing ring with the undercut structure at 26°C and 40°C. The tuning efficiency is found to be 3479.5 pm/mW and 3480.4 pm/mW, respectively which is greatly enhanced but still has very weak temperature dependence. The measured electrical power values corresponding to the maximum output optical power at different temperatures are summarized in Fig. 7(b). The sensitivity is linearly fitted to be −0.0057 mW/°C, which is one order of magnitude smaller. It is also possible to further reduce the temperature sensitivity by tuning the dimensions of one or both rings to make them have much closer resonance wavelength temperature sensitivity, however both optical and thermal properties of the biochemical samples have to be characterized first and considered in the design carefully.

In summary, we have studied the thermal property of the electrical tracing-assisted dual-microring optical sensor. Its temperature sensitivity is found to be ~6 times lower than that of a single ring optical sensor, which is attributed to the compensation of the temperature dependence of the sensing ring with the tracing ring. The electrical tuning efficiency is found to be not sensitive to temperature change and the temperature sensitivity in terms of electrical power per degree for two kinds of electrode heater has been measured. Together with the feature of using cheaper broadband light source instead of a bulky and expensive wavelength-tunable laser, this new type of electrical tracing-assisted dual-microring sensors with low temperature dependence has great potential to be deployed in various practical point-of-care diagnostic applications.

Acknowledgments

This work was supported by the Agency for Science Technology and Research (A*STAR) Joint Council Office (JCO) grant (1234e00018), Singapore.

#220696 - $15.00 USD Received 11 Aug 2014; revised 18 Sep 2014; accepted 19 Sep 2014; published 23 Oct 2014